

Realistic Shell Model Study of Electroweak Decays: a Chiral Perturbation Theory Approach

Nunzio Itaco

Università della Campania “Luigi Vanvitelli”
Istituto Nazionale di Fisica Nucleare - Sezione di Napoli

Electroweak Physics InterseCtions - EPIC 2024



Quenching of $\sigma\tau$ matrix elements

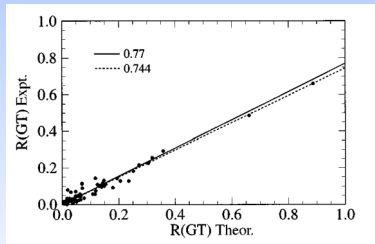
Quenching of $\sigma\tau$ matrix elements is quite a general phenomenon in nuclear-structure physics.

Gamow-Teller transitions (β -decay, EC , $2\nu\beta\beta$, charge-exchange) are hindered from expected values based on sum rules derived by nuclear structure models.

Quenching of $\sigma\tau$ matrix elements

Quenching of $\sigma\tau$ matrix elements is quite a general phenomenon in nuclear-structure physics.

Gamow-Teller transitions (β -decay, EC , $2\nu\beta\beta$, charge-exchange) are hindered from expected values based on sum rules derived by nuclear structure models.

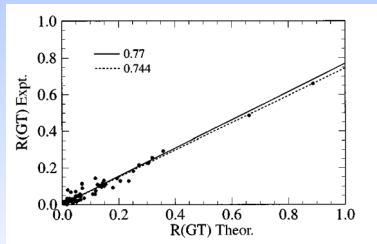


V: G. Martinez Pinedo et al., Phys. Rev. C 53, R2602 (1996)
Università
degli Studi
della Campania
Luigi Vanvitelli

Quenching of $\sigma\tau$ matrix elements

Quenching of $\sigma\tau$ matrix elements is quite a general phenomenon in nuclear-structure physics.

Gamow-Teller transitions (β -decay, EC , $2\nu\beta\beta$, charge-exchange) are hindered from expected values based on sum rules derived by nuclear structure models.



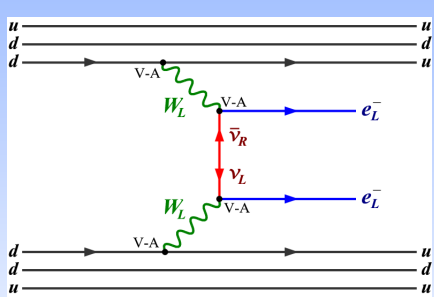
$$g_A \Rightarrow g_A^{\text{eff}} = q g_A$$

J. T. Suhonen
Frontiers in Physics 5, 55 (2017)

Quenching of $\sigma\tau$ matrix elements & $0\nu\beta\beta$ decay

The inverse of the $0\nu\beta\beta$ -decay half-life is proportional to the squared nuclear matrix element (NME).

This evidences the relevance to calculate the NME



$$\left[T_{1/2}^{0\nu} \right]^{-1} = G^{0\nu} \left| M^{0\nu} \right|^2 \langle m_\nu \rangle^2 \propto g_A^4$$

- $G^{0\nu}$ → phase-space factor
- $\langle m_\nu \rangle = \left| \sum_k m_k U_{ek}^2 \right|$
effective mass of the Majorana neutrino, U_{ek}
being the lepton mixing matrix

Quenching of $\sigma\tau$ matrix elements: theory

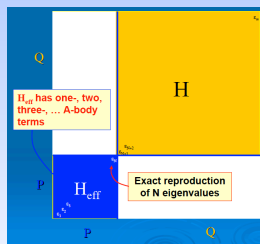
Two main sources \Rightarrow missing degrees of freedom

Quenching of $\sigma\tau$ matrix elements: theory

Two main sources \Rightarrow missing degrees of freedom

Limited model space

Nuclear-structure calculations are carried out in truncated model spaces \Rightarrow effective Hamiltonians and operators



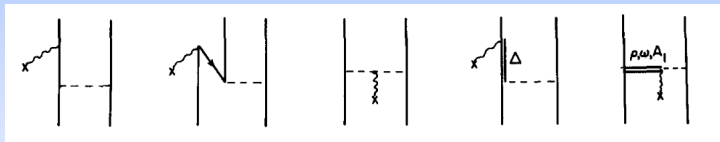
The diagram shows six different effective operators (O_h) represented by arrows pointing upwards. Each operator has a vertical arrow with a double-headed arrow below it, labeled b at the top and a at the bottom. The operators are arranged horizontally and include various combinations of dashed and solid lines, and arrows pointing in different directions.

Quenching of $\sigma\tau$ matrix elements: theory

Two main reasons \Rightarrow missing degrees of freedom

Non-nucleonic degrees of freedom

Processes in which the weak probe prompts a meson to be exchanged between two nucleons \Rightarrow meson-exchange two-body currents (2BC)



H. Hyuga and A. Arima, J. Phys. Soc. Jpn. Suppl. 34, 538 (1973)

Quenching of $\sigma\tau$ matrix elements: truncated model space

Reduced model space P

$$H \Rightarrow H_{\text{eff}}$$

$$H|\Psi_\nu\rangle = E_\nu|\Psi_\nu\rangle \Rightarrow H_{\text{eff}}|\Phi_\alpha\rangle = E_\alpha|\Phi_\alpha\rangle$$

$|\Phi_\alpha\rangle$ = eigenvectors obtained diagonalizing H_{eff} in the reduced model space $\Rightarrow |\Phi_\alpha\rangle = P|\Psi_\alpha\rangle$

$$\langle\Phi_\alpha|\hat{\Theta}|\Phi_\beta\rangle \neq \langle\Psi_\alpha|\hat{\Theta}|\Psi_\beta\rangle$$

Quenching of $\sigma\tau$ matrix elements: truncated model space

Reduced model space P

$$H \Rightarrow H_{\text{eff}}$$

$$H|\Psi_\nu\rangle = E_\nu|\Psi_\nu\rangle \Rightarrow H_{\text{eff}}|\Phi_\alpha\rangle = E_\alpha|\Phi_\alpha\rangle$$

$|\Phi_\alpha\rangle$ = eigenvectors obtained diagonalizing H_{eff} in the reduced model space $\Rightarrow |\Phi_\alpha\rangle = P|\Psi_\alpha\rangle$

$$\langle\Phi_\alpha|\hat{\Theta}|\Phi_\beta\rangle \neq \langle\Psi_\alpha|\hat{\Theta}|\Psi_\beta\rangle$$

Quenching of $\sigma\tau$ matrix elements: truncated model space

Effective operator $\hat{\Theta}_{\text{eff}}$: definition

$$\langle \Phi_\alpha | \hat{\Theta}_{\text{eff}} | \Phi_\beta \rangle = \langle \Psi_\alpha | \hat{\Theta} | \Psi_\beta \rangle$$

$$\hat{\Theta}_{\text{eff}} = \sum_{\alpha\beta} |\Phi_\alpha\rangle\langle\Psi_\alpha| \hat{\Theta} |\Psi_\beta\rangle\langle\Phi_\beta|$$

Quenching of $\sigma\tau$ matrix elements: truncated model space

Effective operator $\hat{\Theta}_{\text{eff}}$: definition

$$\langle \Phi_\alpha | \hat{\Theta}_{\text{eff}} | \Phi_\beta \rangle = \langle \Psi_\alpha | \hat{\Theta} | \Psi_\beta \rangle$$

$$\hat{\Theta}_{\text{eff}} = \sum_{\alpha\beta} |\Phi_\alpha\rangle\langle\Psi_\alpha| \hat{\Theta} |\Psi_\beta\rangle\langle\Phi_\beta|$$

Gamow-Teller operator

$$\hat{\Theta}^{GT} = g_A \sigma \tau^\pm \Rightarrow \hat{\Theta}_{\text{eff}}^{GT} = g_A^{\text{eff}} \sigma \tau^\pm$$

Quenching of $\sigma\tau$ matrix elements: truncated model space

Effective operator $\hat{\Theta}_{\text{eff}}$: definition

$$\langle \Phi_\alpha | \hat{\Theta}_{\text{eff}} | \Phi_\beta \rangle = \langle \Psi_\alpha | \hat{\Theta} | \Psi_\beta \rangle$$

$$\hat{\Theta}_{\text{eff}} = \sum_{\alpha\beta} |\Phi_\alpha\rangle\langle\Psi_\alpha| \hat{\Theta} |\Psi_\beta\rangle\langle\Phi_\beta|$$

Gamow-Teller operator

$$\hat{\Theta}^{GT} = g_A \sigma \tau^\pm \Rightarrow \hat{\Theta}_{\text{eff}}^{GT} = g_A^{\text{eff}} \sigma \tau^\pm$$

Electric quadrupole operator

$$\hat{\Theta}^{E2} = e r^2 Y_\mu^2 \Rightarrow \hat{\Theta}_{\text{eff}}^{E2} = e^{\text{eff}} r^2 Y_\mu^2$$



Quenching of $\sigma\tau$ matrix elements: meson exchange currents

- In the 80s starting from OBEP models two-nucleon meson-exchange current operators have been constructed consistently as required by the continuity equation for vector currents and the PCAC.
- Nowadays, EFT provides a powerful approach where both nuclear potentials and two-body electroweak currents (2BC) may be consistently constructed, the latter appearing as subleading corrections to the one-body GT operator $\sigma\tau^\pm$



Università
degli Studi
della Campania
Luigi Vanvitelli

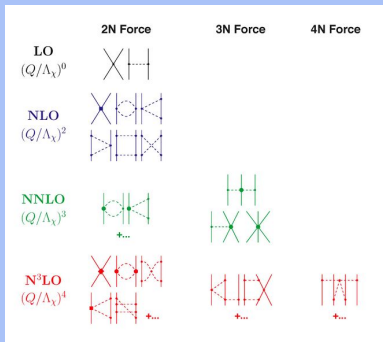
Quenching of $\sigma\tau$ matrix elements: meson exchange currents

- In the 80s starting from OBEP models two-nucleon meson-exchange current operators have been constructed consistently as required by the continuity equation for vector currents and the PCAC.
- Nowadays, EFT provides a powerful approach where both nuclear potentials and two-body electroweak currents (2BC) may be consistently constructed, the latter appearing as subleading corrections to the one-body GT operator $\sigma\tau^\pm$

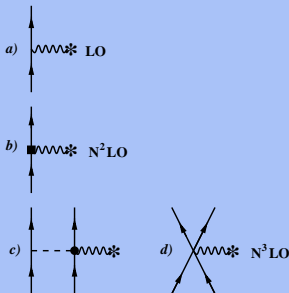
Quenching of $\sigma\tau$ matrix elements: meson exchange currents

- Nowadays, EFT provides a powerful approach where both nuclear potentials and two electroweak currents may be consistently constructed, the latter appearing as subleading corrections to the one-body GT operator $\sigma\tau^\pm$

Nuclear potential

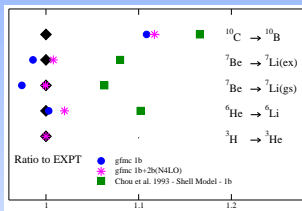


Electroweak axial currents

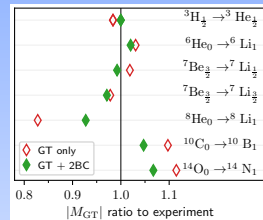


Two-body e.w. currents effects: light nuclei

GT nuclear matrix elements of the β -decay of p -shell nuclei have been calculated with Quantum Monte Carlo (QMC) and no-core shell model (NCSM) methods, including contributions from 2BC

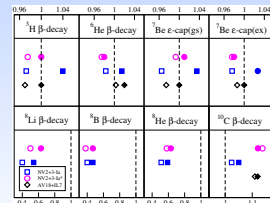


S. Pastore et al., Phys. Rev. C 97 022501(R) (2018)



P. Gysbers et al., Nat. Phys. 15 428 (2019)

The contribution of 2BC improves systematically the agreement between theory and experiment



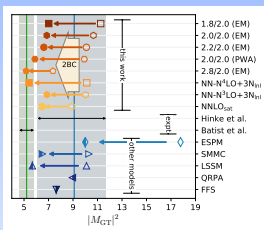
G. B. King et al., Phys. Rev. C 102 025501 (2020)



Università
degli Studi
della Campania
Luigi Vanvitelli

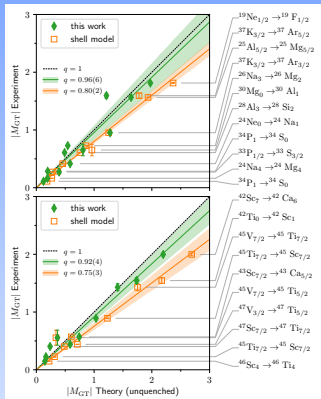
Two-body e.w. currents effects: medium mass nuclei

Coupled-cluster method **CCM** and in-medium SRG (**IMRSG**) calculations have recently performed to overcome the quenching problem g_A to reproduce β -decay observables in heavier systems
P. Gysbers et al., Nat. Phys. 15 428 (2019)



Coupled-Cluster Method

A proper treatment of nuclear correlations and consistency between GT two-body currents and 3N forces, derived in terms of **ChPT**, describes microscopically the “quenching puzzle”



In-Medium SRG

Realistic Shell-Model Calculations

Realistic shell-model calculations starting from a nuclear Hamiltonian and electroweak axial currents derived consistently by way of χ PT.

Università "Vanvitelli" and
INFN-Napoli

- L. Coraggio
- G. De Gregorio
- A. Gargano
- N. I.

INFN-Pisa

- M. Viviani

Peking University

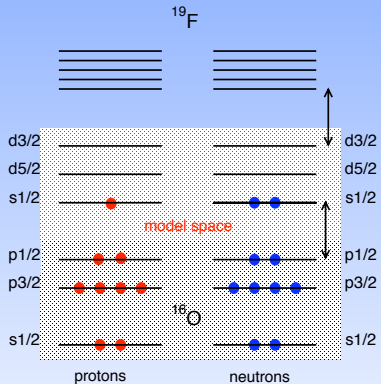
- Z. H. Cheng
- Y. Z. Ma
- F. R. Xu



Università
degli Studi
della Campania
Luigi Vanvitelli

Realistic Shell-Model Calculations

Shell model \Rightarrow well-established approach to obtain a microscopic description of both collective and single-particle properties of nuclei



The degrees of freedom of the core nucleons and the excitations of the valence ones above the model space are not considered explicitly.

$$V_{NN} \ (+ V_{NNN}) \Rightarrow \text{many-body theory} \Rightarrow H_{\text{eff}}$$



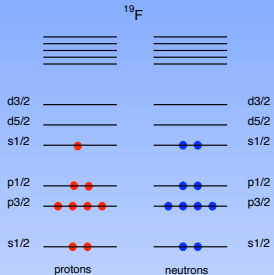
Università
degli Studi
della Campania
Luigi Vanvitelli

Effective shell-model hamiltonian

A-nucleon system Schrödinger equation

$$H|\Psi_\nu\rangle = E_\nu|\Psi_\nu\rangle$$

$$H = H_0 + H_1 = \sum_{i=1}^A (T_i + U_i) + \sum_{i < j} (V_{ij}^{NN} - U_i)$$



Effective shell-model hamiltonian

A-nucleon system Schrödinger equation

$$H|\Psi_\nu\rangle = E_\nu|\Psi_\nu\rangle$$

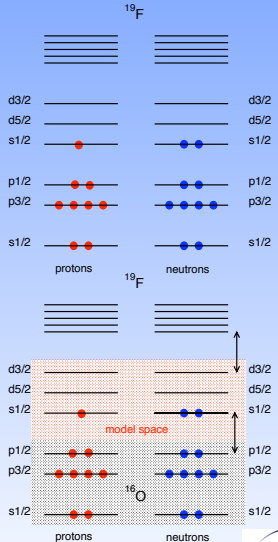
$$H = H_0 + H_1 = \sum_{i=1}^A (T_i + U_i) + \sum_{i < j} (V_{ij}^{NN} - U_i)$$

Model space

$$|\Phi_i\rangle = [a_1^\dagger a_2^\dagger \dots a_n^\dagger]_i |c\rangle \Rightarrow P = \sum_{i=1}^d |\Phi_i\rangle\langle\Phi_i|$$

Model-space eigenvalue problem

$$H_{\text{eff}} P |\Psi_\alpha\rangle = E_\alpha P |\Psi_\alpha\rangle$$



Effective shell-model Hamiltonian

$$\left(\begin{array}{c|c} PHP & PHQ \\ \hline QHP & QHQ \end{array} \right) \quad \mathcal{H} = \Omega^{-1} H \Omega \quad \Rightarrow \quad \left(\begin{array}{c|c} P\mathcal{H}P & P\mathcal{H}Q \\ \hline 0 & Q\mathcal{H}Q \end{array} \right)$$

$Q\mathcal{H}P = 0$

$$H_{\text{eff}} = P\mathcal{H}P$$

$$\text{Suzuki \& Lee} \Rightarrow \Omega = e^\omega \text{ with } \omega = \left(\begin{array}{c|c} 0 & 0 \\ \hline Q\omega P & 0 \end{array} \right)$$

$$H_1^{\text{eff}}(\omega) = PH_1P + PH_1Q \frac{1}{\epsilon - QHQ} QH_1P - PH_1Q \frac{1}{\epsilon - QHQ} \omega H_1^{\text{eff}}(\omega)$$

The shell-model effective hamiltonian

Folded-diagram expansion

\hat{Q} -box vertex function

$$\hat{Q}(\epsilon) = PH_1P + PH_1Q\frac{1}{\epsilon - QHQ}QH_1P$$

\Rightarrow Recursive equation for H_{eff} \Rightarrow iterative techniques
(Krenciglowa-Kuo, Lee-Suzuki, ...)

$$H_{\text{eff}} = \hat{Q} - \hat{Q}' \int \hat{Q} + \hat{Q}' \int \hat{Q} \int \hat{Q} - \hat{Q}' \int \hat{Q} \int \hat{Q} \int \hat{Q} \dots ,$$

generalized folding

The perturbative approach to the shell-model H^{eff}

$$\hat{Q}(\epsilon) = PH_1P + PH_1Q\frac{1}{\epsilon - QHQ}QH_1P$$

The \hat{Q} -box can be calculated perturbatively

$$\frac{1}{\epsilon - QHQ} = \sum_{n=0}^{\infty} \frac{(QH_1Q)^n}{(\epsilon - QH_0Q)^{n+1}}$$

The diagrammatic expansion of the \hat{Q} -box

The perturbative approach to the shell-model H^{eff}

$$\hat{Q}(\epsilon) = PH_1P + PH_1Q\frac{1}{\epsilon - QHQ}QH_1P$$

The \hat{Q} -box can be calculated perturbatively

$$\frac{1}{\epsilon - QHQ} = \sum_{n=0}^{\infty} \frac{(QH_1Q)^n}{(\epsilon - QH_0Q)^{n+1}}$$

The diagrammatic expansion of the \hat{Q} -box

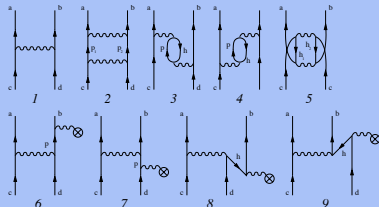
The perturbative approach to the shell-model H^{eff}

$$\hat{Q}(\epsilon) = PH_1P + PH_1Q\frac{1}{\epsilon - QHQ}QH_1P$$

The \hat{Q} -box can be calculated perturbatively

$$\frac{1}{\epsilon - QHQ} = \sum_{n=0}^{\infty} \frac{(QH_1Q)^n}{(\epsilon - QH_0Q)^{n+1}}$$

The diagrammatic expansion of the \hat{Q} -box



The shell-model effective operators

$\hat{\Theta}_{\text{eff}}$ can be derived consistently in the MBPT framework

The shell-model effective operators

$\hat{\Theta}_{\text{eff}}$ can be derived consistently in the MBPT framework

$$\Theta_{\text{eff}} = (P + \hat{Q}_1 + \hat{Q}_1 \hat{Q}_1 + \hat{Q}_2 \hat{Q} + \hat{Q} \hat{Q}_2 + \dots)(\chi_0 + \chi_1 + \chi_2 + \dots)$$

where the functions χ_n are defined as

$$\chi_0 = (\hat{\Theta}_0 + h.c.) + \Theta_{00} ,$$

$$\chi_1 = (\hat{\Theta}_1 \hat{Q} + h.c.) + (\hat{\Theta}_{01} \hat{Q} + h.c.) ,$$

...

in terms of the vertex functions and their derivatives

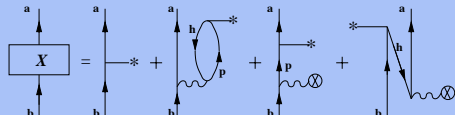
$$\hat{\Theta}(\epsilon) = P\Theta P + P\Theta Q \frac{1}{\epsilon - QHQ} QH_1 P ,$$

$$\hat{\Theta}(\epsilon_1, \epsilon_2) = PH_1 Q \frac{1}{\epsilon_1 - QHQ} Q\Theta Q \frac{1}{\epsilon_2 - QHQ} QH_1 P$$

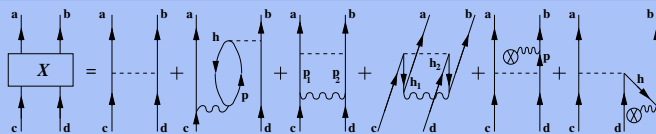
The shell-model effective operators

$\hat{\Theta}_{\text{eff}}$ can be derived consistently in the MBPT framework

One-body operator



Two-body operator



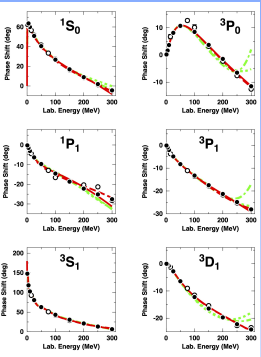
K. Suzuki and R. Okamoto, Prog. Theor. Phys. 93 , 905 (1995)



Università
degli Studi
della Campania
Luigi Vanvitelli

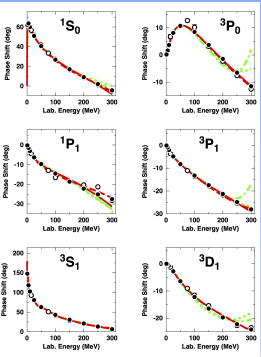
Realistic Shell-Model Calculations

- Nuclear Hamiltonian:
Entem-Machleidt N^3LO two-body potential plus N^2LO three-body potential ($\Lambda = 500$ MeV)
- Axial current J_A calculated at N^3LO in ChPT
- H_{eff} obtained calculating the Q -box up to the 3rd order in V_{NN} (up to 2p-2h core excitations) and up to the 1st order in V_{NNN}
- Effective operators are consistently derived by way of the MBPT



Realistic Shell-Model Calculations

- Nuclear Hamiltonian:
Entem-Machleidt N^3LO two-body potential plus N^2LO three-body potential ($\Lambda = 500$ MeV)
- Axial current J_A calculated at N^3LO in ChPT
- H_{eff} obtained calculating the Q -box up to the 3rd order in V_{NN} (up to 2p-2h core excitations) and up to the 1st order in V_{NNN}
- Effective operators are consistently derived by way of the MBPT



The axial current \mathbf{J}_A

The matrix elements of the axial current \mathbf{J}_A are derived through a chiral expansion up to **N³LO**, and employing the same LECs as in **2NF** and **3NF**

$$\mathbf{J}_{A,\pm}^{\text{LO}} = -g_A \sum_i \boldsymbol{\sigma}_i \tau_{i,\pm} ,$$

$$\mathbf{J}_{A,\pm}^{\text{N}^2\text{LO}} = \frac{g_A}{2m_N^2} \sum_i \mathbf{K}_i \times (\boldsymbol{\sigma}_i \times \mathbf{K}_i) \tau_{i,\pm} ,$$

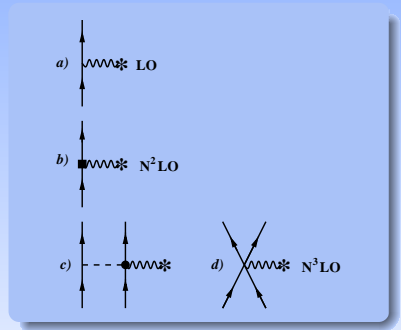
$$\mathbf{J}_{A,\pm}^{\text{N}^3\text{LO}}(1\text{PE}; \mathbf{k}) = \sum_{i < j} \frac{g_A}{2f_\pi^2} \left\{ 4c_3 \tau_{j,\pm} \mathbf{k} + (\boldsymbol{\tau}_i \times \boldsymbol{\tau}_j)_\pm \right.$$

$$\left. \times \left[\left(c_4 + \frac{1}{4m} \boldsymbol{\sigma}_i \times \mathbf{k} - \frac{i}{2m} \mathbf{K}_i \right) \right] \right\} \boldsymbol{\sigma}_j \cdot \mathbf{k} \frac{1}{\omega_k^2} ,$$

$$\mathbf{J}_{A,\pm}^{\text{N}^3\text{LO}}(\text{CT}; \mathbf{k}) = \sum_{i < j} z_0 (\boldsymbol{\tau}_i \times \boldsymbol{\tau}_j)_\pm (\boldsymbol{\sigma}_i \times \boldsymbol{\sigma}_j) ,$$

where

$$z_0 = \frac{g_A}{2f_\pi^2 m_N} \left[\frac{m_N}{4g_A \Lambda_\chi} c_D + \frac{m_N}{3} (c_3 + 2c_4) + \frac{1}{6} \right] .$$



A. Baroni, L. Girlanda, S. Pastore, R. Schiavilla, and M. Viviani,
Phys. Rev. C 93, 015501 (2016)



Università
degli Studi
della Campania
Luigi Vanvitelli

The axial current \mathbf{J}_A

The matrix elements of the axial current \mathbf{J}_A are derived through a chiral expansion up to N^3LO , and employing the same LECs as in 2NF and 3NF

$$\mathbf{J}_{A,\pm}^{\text{LO}} = -g_A \sum_i \boldsymbol{\sigma}_i \tau_{i,\pm} ,$$

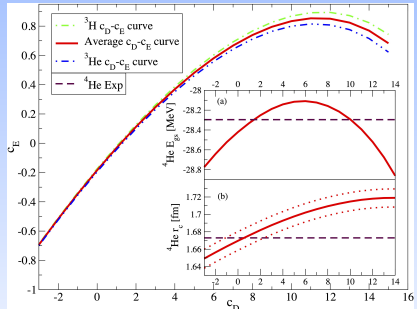
$$\mathbf{J}_{A,\pm}^{N^2\text{LO}} = \frac{g_A}{2m_N^2} \sum_i \mathbf{K}_i \times (\boldsymbol{\sigma}_i \times \mathbf{K}_i) \tau_{i,\pm} ,$$

$$\begin{aligned} \mathbf{J}_{A,\pm}^{N^3\text{LO}}(1\text{PE}; \mathbf{k}) &= \sum_{i < j} \frac{g_A}{2f_\pi^2} \left\{ 4\mathbf{c}_3 \tau_{j,\pm} \mathbf{k} + (\boldsymbol{\tau}_i \times \boldsymbol{\tau}_j)_\pm \right. \\ &\quad \times \left[\left(\mathbf{c}_4 + \frac{1}{4m} \boldsymbol{\sigma}_i \times \mathbf{k} - \frac{i}{2m} \mathbf{K}_i \right) \right] \left. \right\} \boldsymbol{\sigma}_j \cdot \mathbf{k} \frac{1}{\omega_k^2} , \end{aligned}$$

$$\mathbf{J}_{A,\pm}^{N^3\text{LO}}(\text{CT}; \mathbf{k}) = \sum_{i < j} z_0 (\boldsymbol{\tau}_i \times \boldsymbol{\tau}_j)_\pm (\boldsymbol{\sigma}_i \times \boldsymbol{\sigma}_j) ,$$

where

$$z_0 = \frac{g_A}{2f_\pi^2 m_N} \left[\frac{m_N}{4g_a \Lambda_\chi} \mathbf{c}_D + \frac{m_N}{3} (\mathbf{c}_3 + 2\mathbf{c}_4) + \frac{1}{6} \right] .$$

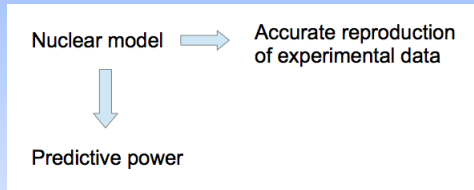


Realistic Shell-Model Calculations

- *fp*-shell nuclei: four proton and neutron orbitals outside *LS* core
 $^{40}\text{Ca} \rightarrow 0f_{7/2}, 0f_{5/2}, 1p_{3/2}, 1p_{1/2}$
- *fpg*-shell nuclei: four proton and neutron orbitals outside *jj* core
 $^{56}\text{Ni} \rightarrow 0f_{5/2}, 1p_{3/2}, 1p_{1/2}, 0g_{9/2}$

Realistic Shell-Model Calculations

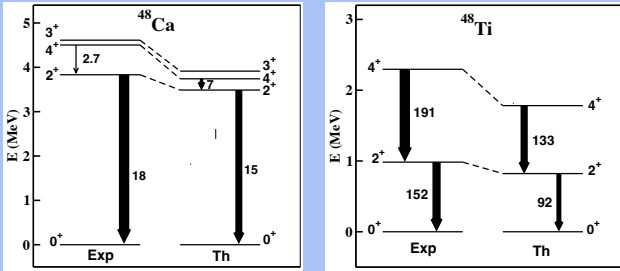
- *fp*-shell nuclei: four proton and neutron orbitals outside *LS* core
 $^{40}\text{Ca} \rightarrow 0f_{7/2}, 0f_{5/2}, 1p_{3/2}, 1p_{1/2}$
- *fpg*-shell nuclei: four proton and neutron orbitals outside *jj* core
 $^{56}\text{Ni} \rightarrow 0f_{5/2}, 1p_{3/2}, 1p_{1/2}, 0g_{9/2}$



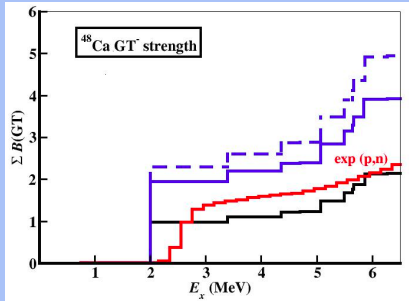
RSM calculations, starting from ChPT two- and three-body potentials and two-body electroweak currents for spectroscopic and spin-isospin dependent observables of ^{48}Ca , ^{76}Ge , ^{82}Se

L. Coraggio, N. Itaco, G. De Gregorio, A. Gargano, Z. H. Cheng, Y. Z. Ma, F. R. Xu, and M. Viviani, Phys. Rev. C 109, 014301 (2024)

fp-shell nuclei: spectroscopic properties



^{48}Ca GT strength distribution



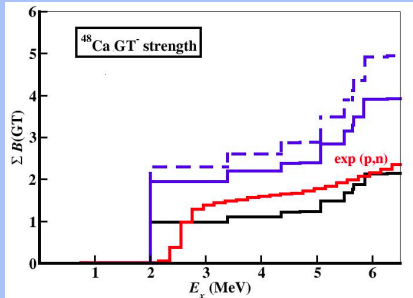
Charge-exchange experiments

$$\left[\frac{d\sigma}{d\Omega}(q=0) \right] = \hat{\sigma} B_{\text{exp}}(\text{GT})$$

$$B_{\text{Th}}(\text{GT}) = \frac{|\langle \Phi_f || \mathbf{J}_A || \Phi_i \rangle|^2}{2J_i + 1}$$

- bare \mathbf{J}_A at LO in ChPT
(namely the GT operator $g_A \boldsymbol{\sigma} \cdot \boldsymbol{\tau}$)
- effective \mathbf{J}_A at LO in ChPT
- effective \mathbf{J}_A at N³LO in ChPT

^{48}Ca GT strength distribution



Charge-exchange experiments

$$\left[\frac{d\sigma}{d\Omega}(q=0) \right] = \hat{\sigma} B_{\text{exp}}(GT)$$

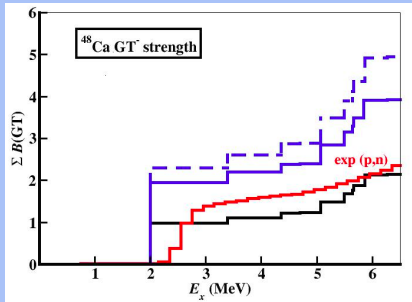
$$B_{\text{Th}}(GT) = \frac{|\langle \Phi_f || \mathbf{J}_A || \Phi_i \rangle|^2}{2J_i + 1}$$

- bare \mathbf{J}_A at LO in ChPT
(namely the GT operator $g_A \boldsymbol{\sigma} \cdot \boldsymbol{\tau}$)
- effective \mathbf{J}_A at LO in ChPT
- effective \mathbf{J}_A at $N^3\text{LO}$ in ChPT

Total GT^- strength

	(a)	(b)	(c)	Expt
$\sum B(GT^-)$	24.0	17.5	11.2	15.3 ± 2.2

^{48}Ca GT strength distribution

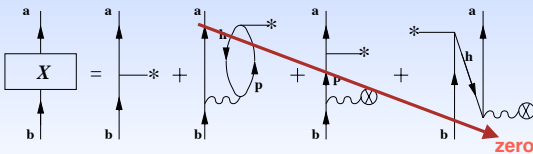


Charge-exchange experiments

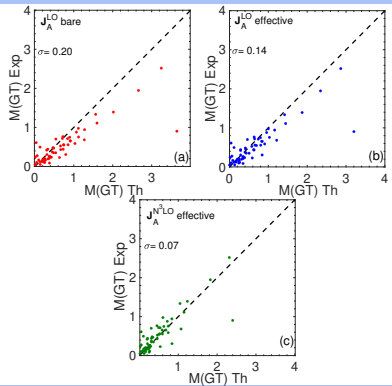
$$\left[\frac{d\sigma}{d\Omega}(q=0) \right] = \hat{\sigma} B_{exp}(GT)$$

$$B_{Th}(GT) = \frac{|\langle \Phi_f || \mathbf{J}_A || \Phi_i \rangle|^2}{2J_i + 1}$$

--- bare \mathbf{J}_A at LO in ChPT
 (namely the GT operator $g_A \boldsymbol{\sigma} \cdot \boldsymbol{\tau}$)
 —— effective \mathbf{J}_A at LO in ChPT
 — effective \mathbf{J}_A at N^3LO in ChPT



fp-shell nuclei: GT matrix elements



GT matrix elements of 60 experimental decays of 43 *fp*-shell nuclei

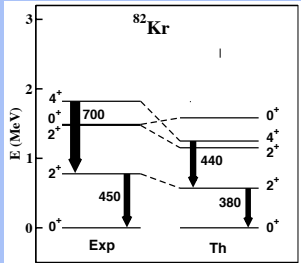
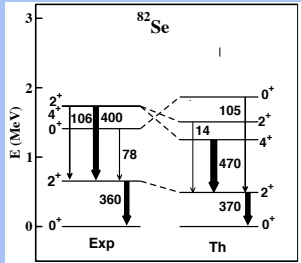
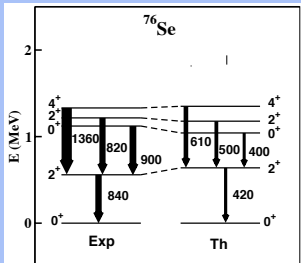
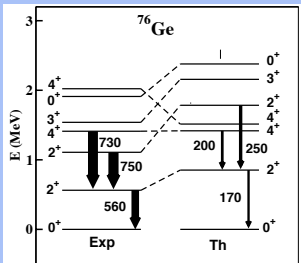
- (a) bare J_A at LO in ChPT (namely the GT operator $g_A \boldsymbol{\sigma} \cdot \boldsymbol{\tau}$);
- (b) effective J_A at LO in ChPT;
- (c) effective J_A at $N^3\text{LO}$ in ChPT.

$$\sigma = \sqrt{\frac{\sum_{i=1}^n (x_i - \hat{x}_i)^2}{n}}$$

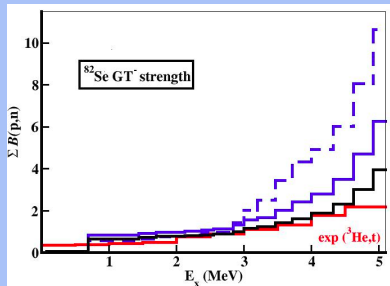
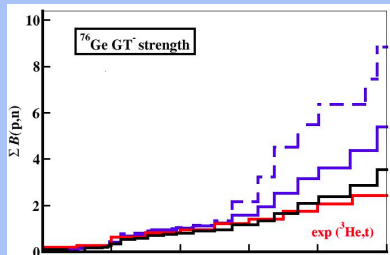
$$\frac{(a)}{\sigma} \quad 0.20 \quad \rightarrow \quad \frac{(b)}{0.14} \quad \rightarrow \quad \frac{(d)}{0.07}$$



$0f_{5/2}1p_0g_{9/2}$ -shell nuclei spectroscopic properties



^{76}Ge & ^{82}Se GT strength distributions



Charge-exchange experiments

$$\left[\frac{d\sigma}{d\Omega}(q=0) \right] = \hat{\sigma} B_{\text{exp}}(GT)$$

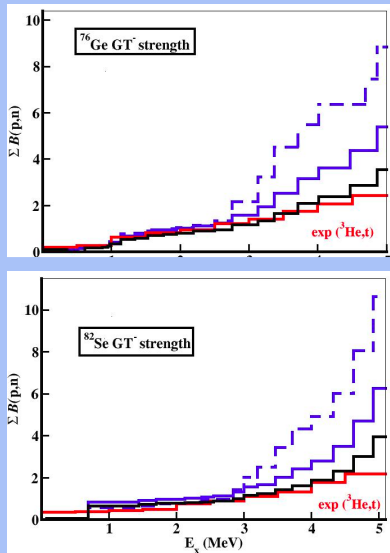
$$B_{\text{Th}}(GT) = \frac{|\langle \Phi_f | |\mathbf{J}_A| | \Phi_i \rangle|^2}{2J_i + 1}$$

- bare \mathbf{J}_A at LO in ChPT
(namely the GT operator $g_A \boldsymbol{\sigma} \cdot \boldsymbol{\tau}$)
- effective \mathbf{J}_A at LO in ChPT
- effective \mathbf{J}_A at N³LO in ChPT



Università
degli Studi
della Campania
Luigi Vanvitelli

^{76}Ge & ^{82}Se GT strength distributions



Charge-exchange experiments

$$\left[\frac{d\sigma}{d\Omega}(q=0) \right] = \hat{\sigma} B_{exp}(GT)$$

$$B_{Th}(GT) = \frac{|\langle \Phi_f || \mathbf{J}_A || \Phi_i \rangle|^2}{2J_i + 1}$$

- bare \mathbf{J}_A at LO in ChPT
(namely the GT operator $g_A \boldsymbol{\sigma} \cdot \boldsymbol{\tau}$)
- effective \mathbf{J}_A at LO in ChPT
- effective \mathbf{J}_A at N³LO in ChPT

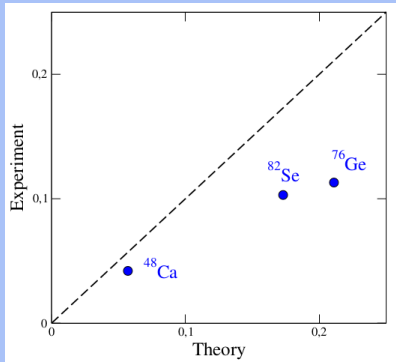
Total GT⁻ strength

	(a)	(b)	(c)	Expt
^{76}Ge	15.8	10.6	7.1	~
^{82}Se	19.0	11.9	7.6	~



$2\nu\beta\beta$ nuclear matrix elements

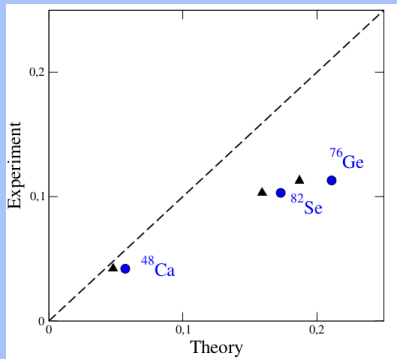
$$M_{2\nu}^{\text{GT}} = \sum_n \frac{\langle 0_f^+ || \mathbf{J}_A || 1_n^+ \rangle \langle 1_n^+ || \mathbf{J}_A || 0_i^+ \rangle}{E_n + E_0}$$



Blue dots:
bare \mathbf{J}_A at LO in ChPT (namely
the GT operator $g_A \boldsymbol{\sigma} \cdot \boldsymbol{\tau}$)

$2\nu\beta\beta$ nuclear matrix elements

$$M_{2\nu}^{\text{GT}} = \sum_n \frac{\langle 0_f^+ || \mathbf{J}_A || 1_n^+ \rangle \langle 1_n^+ || \mathbf{J}_A || 0_i^+ \rangle}{E_n + E_0}$$



Blue dots:

bare \mathbf{J}_A at LO in ChPT (namely the GT operator $g_A \sigma \cdot \tau$)

Black triangles:

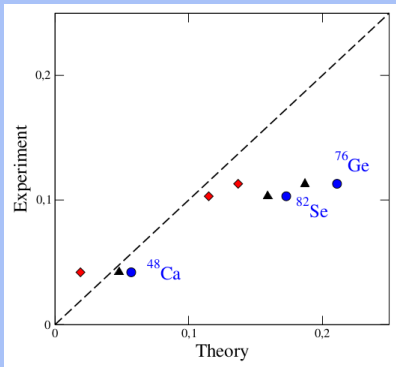
effective \mathbf{J}_A at LO in ChPT



Università
degli Studi
della Campania
Luigi Vanvitelli

$2\nu\beta\beta$ nuclear matrix elements

$$M_{2\nu}^{\text{GT}} = \sum_n \frac{\langle 0_f^+ || \mathbf{J}_A || 1_n^+ \rangle \langle 1_n^+ || \mathbf{J}_A || 0_i^+ \rangle}{E_n + E_0}$$



Blue dots:

bare \mathbf{J}_A at LO in ChPT (namely the GT operator $g_A \sigma \cdot \tau$)

Black triangles:

effective \mathbf{J}_A at LO in ChPT

Red diamonds:

effective \mathbf{J}_A at N³LO in ChPT



Università
degli Studi
della Campania
Luigi Vanvitelli

Conclusions & Perspectives

- Correlations + electroweak 2BC \Rightarrow quite good description of $\sigma\tau$ observables
 - 2BC introduce $\simeq 20\%$ reduction of GT matrix elements
-
- Two-body currents for the $M1$ transitions
 - Calculations for heavier-mass systems (^{100}Mo , ^{130}Te , ^{136}Xe)
 - Calculating $0\nu\beta\beta$ decay $M^{0\nu}$ in the same χPT framework:
LO contact term, three-body currents, ..



Conclusions & Perspectives

- Correlations + electroweak 2BC \Rightarrow quite good description of $\sigma\tau$ observables
 - 2BC introduce $\simeq 20\%$ reduction of GT matrix elements
-
- Two-body currents for the $M1$ transitions
 - Calculations for heavier-mass systems (^{100}Mo , ^{130}Te , ^{136}Xe)
 - Calculating $0\nu\beta\beta$ decay $M^{0\nu}$ in the same χPT framework:
LO contact term, three-body currents, ..



Question for the discussion

- Is it possible to robustly quantify the error due to the truncation in the EFT expansion?

Realistic Shell Model Study of Electroweak Decays: a Chiral Perturbation Theory Approach

Nunzio Itaco

Università della Campania “Luigi Vanvitelli”
Istituto Nazionale di Fisica Nucleare - Sezione di Napoli

Electroweak Physics InterseCtions - EPIC 2024

